



**Environmental
Science**
Nano

Persistent arsenate – iron(III) oxyhydroxide – organic matter nanoaggregates observed in coals

Journal:	<i>Environmental Science: Nano</i>
Manuscript ID	EN-ART-06-2021-000502.R2
Article Type:	Paper

SCHOLARONE™
Manuscripts

Environmental significance

The biogeochemical behavior of As is largely affected by redox-based transformation of Fe minerals that are very redox-sensitive. While lab studies have proven that natural organic matter (NOM) is able to affect the transformation of Fe minerals and thus those associated As, very limited conclusion is drawn in the practical reducing environment such as coal beds, marine sediments and aquifers where both NOM and "As-Fe" system exist. Our study showed the existence of oxidizing As and Fe species that are supposed to be reduced in coals. We, at nano-scale, found the preservation effect of NOM should be responsible for the "As(V)-Fe(III)" system in coals based on spectroscopic evidence. Thus, our study shed lights on nano-scale mechanisms of how NOM can interact and then affect the Fe oxyhydroxide-arsenate system in practical reducing environment.

ARTICLE

Persistent arsenate – iron(III) oxyhydroxide – organic matter nanoaggregates observed in coals

Yinfeng Zhang^{ab}, Shehong Li^b, Jing Sun^b, Benjamin C. Bostick^c, and Yan Zheng^{de*}

Received 18th May 2021,
Accepted 00th xxxx 2021

DOI: 10.1039/x0xx00000x

Abstract : How natural nanoaggregates of iron (Fe) and organic matter (OM), currently identified in organic rich soil or peat, interact with metals and metalloids is environmentally significant. Coal is also organic-rich and exemplifies anoxic sedimentary environment with Fe usually as pyrite not oxides. Here, we analyze the local structure of Fe (6,880-21,700 mg/kg) and As (45-5680 mg/kg) in representative Guizhou coals using X-ray absorption near-edge and fine-structure spectroscopy (XANES and EXAFS) to illustrate how Fe(III) and As(V) is preserved in coals formed from reduced, organic-rich precursors. Arsenic XANES indicate that >80% of As exists as As(V) with <14% of As associated with sulfides in 5 Guizhou coals, confirming published but unexplained results. An As-Fe shell at 3.25-3.29 Å in the As EXAFS suggests that this As(V) is adsorbed to Fe(III) oxyhydroxides as evidenced by Fe EXAFS in these coals. Significantly, the lower Fe-Fe coordination numbers (CN) of 0.6-1.1 relative to that in 2-line ferrihydrite (CN=1.6) and goethite (CN=2.1) suggests these Fe(III) oxyhydroxides are likely Fe-OM nanoaggregates protected by OM encapsulation and adsorption of arsenate. Such structurally stabilized composites of As(V)-Fe(III)-OM may be more widely disseminated and allow oxidized As and Fe to persist in other organic-rich, reducing environments.

1. Introduction

Recent interest in natural nanoaggregates is growing due to their role in controlling the fate of inorganic pollutants in aqueous environment¹⁻⁶. Natural nanoaggregates composed of iron (Fe) and organic matter (OM) have been observed in organic soils and organic soil horizons in wetlands, marine sediments, peatlands and permafrosts⁷⁻¹¹. Because metals and

metalloids have strong affinities for Fe-OM nanoaggregates^{11, 12}, mobilization in response to leaching of soil, thawing of permafrost⁸, and changes in redox conditions¹³ has emerged as transport pathways for pollutants to be reckoned with. Despite the growing environmental significance of Fe-OM nanoaggregates, our understanding of the structural organization and complexation has relied primarily on a series of elegantly designed laboratory studies^{1, 4-6, 14-17}. Molecular level characterization of Fe-OM nanoaggregates and its interaction with metals and metalloids in natural settings remains largely unexplored.

Coal is of interest because the precursor of coal is the organic-rich peat¹⁰, with Fe-OM nanoaggregates identified in coal fly ash¹⁸. A dirty fossil fuel, the global coal consumption for energy production has reached nearly 8 billion tons in 2016¹⁹,

^a Yunnan Key Laboratory of Plateau Wetland Conservation, Restoration and Ecological Services, College of Wetlands, Southwest Forestry University, Kunming, 650224, China.

^b State Key Lab of Environmental Geochemistry, Institute of Geochemistry, Chinese Academy of Sciences, Guiyang, 550081, China.

^c Lamont-Doherty Earth Observatory, Columbia University, 61 Route 9W, Palisades, NY 10964, United States.

^d State Environmental Protection Key Laboratory of Integrated Surface Water-Groundwater Pollution Control, School of Environmental Science and Engineering, Southern University of Science and Technology, Shenzhen, 518055, China

^e Guangdong Provincial Key Laboratory of Soil and Groundwater Pollution Control, School of Environmental Science and Engineering, Southern University of Science and Technology, Shenzhen, 518055, China. Email: yan.zheng@sustech.edu.cn

ORCID: <https://orcid.org/0000-0001-5256-9395>

Electronic Supplementary Information (ESI) available: [ESI available, which contains detailed elemental and mineralogical compositions of coals, map of study area, and LCF results]. See DOI: 10.1039/x0xx00000x

ARTICLE

1
2
3 resulting in an array of environmental problems²⁰. Coal
4 exemplifies highly reduced, organic rich depositional
5 environment that are also rich in toxic metals and metalloids²¹.
6
7
8 It is an ideal natural system to investigate metals/metalloids
9 and Fe-OM interactions, because the subsequent coalification
10 processes that convert peat to coal have resulted in a geologic
11 specimen rich in reduced elements, e.g., carbon and sulfur, in
12 thermodynamic disequilibrium of atmospheric oxygen. The
13 prevailing paradigm about the redox state of metals like Fe and
14 metalloids like As in coal is that much of the Fe and As in coal is
15 bound with pyrite and/or other sulfides, indicative of the anoxic
16 depositional environment during the initial stage of plant burial
17
18
19
20
21
22
23
24
25
26
27
28
29
30
31
32
33
34
35
36
37
38
39
40
41
42
43
44
45
46
47
48
49
50
51
52
53
54
55
56
57
58
59
60

21-25.

At the same time, It is also recognized that As can be associated with organic-rich fractions of coals of widely variable sulfur contents, suggesting that this is not a result of the enrichment of sulfur in organic-rich areas of the specimen²⁶. Sequential leaching of low-S Wyoming coals²⁷, coals from China²⁸, England and Australia²⁹ points to this ubiquitous As-OM association but the nature of it is not well understood. For example, , although small grains and veins of arsenopyrite and As-bearing pyrite have been identified by scanning electron microscope in As-rich (up to 35,000 mg/kg) coals from Guizhou China, the concentration of sulfidic As carrier-phases is inadequate to account for the As abundance on a whole coal basis, prompting the investigators to propose iron oxides and iron phosphate as carrier-phases³⁰. Further, the possibility that OM plays a role is evidenced by the spatially overlapping occurrence of As in Guizhou coal organic matter matrix (see Fig. 3 in Finkelman et al 1999³¹). Curiously, XANES analysis of 12 Guizhou coals have shown the dominance of oxidized As(V),

ranging from 75% to 100%^{32, 33}. Yet how and why coals contain reduced minerals such as pyrite and at the same time As(V) and possibly Fe(III) oxides remains unexplained.

We hypothesize that Fe(III) and As(V) may occur in coal by the formation of As-Fe-OM complexes that involve Fe-OM nanoaggregates to provide a structural protection mechanism against reduction in anoxic depositional environment, with the stability of Fe-OM nanoaggregates enhanced by sorption of arsenate. Our hypothesis stems from the growing spectroscopic and structural evidence demonstrating that polyvalent cations such as Fe can connect As and OM and form stable complexes^{14, 15, 34}. In these ternary systems, OM complexation and micellar protection decrease the reactivity of Fe(III) oxyhydroxides, analogous to the stabilization of Fe(III) in ferritin proteins. Arsenate, and potentially phosphate retention on these Fe colloids and small sized aggregates, may also help to stabilize them³⁵.

To test our hypothesis, a suite of freshly collected Guizhou coal samples from the same high-As coal formation previously investigated^{32, 36} and found to contain oxidized As(V)³⁶ are analyzed for their chemical and bulk mineralogical compositions. Five coal samples, representative of high-As Guizhou coals, together with As-Fe-OM aqueous solutions, As and Fe compounds and minerals taken as standard reference minerals, are subject to synchrotron analysis. The speciation and local coordination environments of As and Fe are characterized by XANES and EXAFS^{14, 15, 34}, with data reduction involving shell-fitting or least-squares linear combination fitting through an iterative process. Results suggest that our hypothesis is viable for coal, with implications on mobility of Fe

and As in organic-rich, reducing sedimentary aquifers discussed at last.

2. Materials and Methods

2.1 Coal Samples

Most coals in the world were deposited since the Late Paleozoic (410 to 245 million years before present) during time periods when global productivity was high, in tropical, flooded anoxic environments where plant organic matter was best preserved³⁷. Based on prior studies³⁶, coal samples from the same Late Permian (299 to 251 millions years before present) Longtan Formation in Guizhou Province³⁶ of southwest China (Fig S1) are chosen for sampling. Longtan Formation consists of limestone-bearing anthracite (indicative of the highest coalification temperature and pressure) coal beds in Anlong (Samples C1, C2, C3 and C5) and Xingren (Sample C4) County, Guizhou (Fig S1). These anthracite coals rich in limestone also contain extensive Carlin-type gold deposits rich in As, Hg, Sb and Tl³⁶. All coal samples were collected into polyethylene zip-lock bags and covered with aluminum foil immediately in the field in July 2014. Upon returning to the laboratory on the same day, the samples were refrigerated at 4 °C until analysis also in July 2014. The coal storage method followed the established practice of coal geologists and geochemists^{33, 38-40} (see details in SM1 and Table S1).

2.2 Bulk chemical and mineralogical analyses

An aliquot of coal samples was air dried for analysis. Concentrations of C and S were determined on an Element Analyzer (Elementar, vario MACRO, Germany) as follows: 0.3000 ± 0.0005 g of samples were weighed and wrapped with tin foil then heated to up to 1200 °C for analysis, with a precision of ~0.5%. Concentrations of Fe and As were determined in total acid digests by inductively coupled plasma-optical emission spectroscopy (ICP-OES, Thermo

6000) and hydride-generation atomic fluorescence spectroscopy (HG-AFS, AFS-2100e), respectively. The acid digestion using high-pressure canisters followed an established protocol at the State Key Laboratory of Environmental Geochemistry (SKLEG), Institute of Geochemistry of Chinese Academy of Sciences⁴¹. Briefly, 3 mL of concentrated HNO₃ (trace metal grade) and 1 mL of concentrated HClO₄ (trace metal grade) were added to 0.0500 ± 0.0003 g of solids in Teflon bottles, placed in an oven at 160 °C for 24 h or longer until the digest became clear. The digested samples were then heated on a hot plate to nearly dryness and re-dissolved with 1% HNO₃. Two standard reference materials (SRM) GSS14 (standard soil sample, Fe = 37240 ± 420 mg/kg, As = 6.5 ± 1.3 mg/kg) and GSS16 (standard soil sample, Fe = 31360 ± 350 mg/kg, As = 18 ± 2 mg/kg) were simultaneously digested and analyzed for quality control and assurance, with data within 90-110% of certified value. Bulk mineralogy were obtained through X-ray diffraction analysis (XRD, D/Max-2200) using a protocol as previously described⁴².

2.3 X-ray Absorption Spectroscopy

2.3.1 Standard Reference Materials (SRM)

Mineral As SRMs. Arsenopyrite (FeAsS, As oxidation state As⁰), realgar (AsS), orpiment (As₂S₃, As oxidation state As³⁺), sodium arsenite (NaAsO₂, Sigma-Aldrich, >99%), sodium arsenate heptahydratearsenate (Na₂HAsO₄·6H₂O, Sigma-Aldrich, 99.995%) and scorodite (FeAsO₄·2H₂O), were obtained from the Certified Reference Material Center, China, with their identities confirmed by XRD analysis.

Sorbed As(V) as SRMs. These were prepared by adding small aliquots of As(V) solutions to a variety of inorganic mineral compounds including 2-line ferrihydrite and goethite (listed in Table

S2) acting as inorganic adsorbents (2 g/L suspension density) to reach an initial spiked As concentration of 100 mg/kg, with final pH adjusted to be between 7.0 and 7.5, with details published previously⁴¹. The spectra of these sorbed As(V)-SRMs were collected at the Beijing Synchrotron Radiation Facility (BSRF) in 2013, with details available in a prior study⁴¹, for least-squares linear combination fitting (LCF) in this study. The modified method of Schwertmann and Cornell⁴³ is used to synthesize 2-line ferrihydrite and goethite with details described in SI (SM2).

As(V)-OM and As(V)-Fe(III)-OM complexes as SRMs. These complexes are prepared using the method of Mikutta *et al*⁴⁴ with modifications, with details in ESI (SM3). Standard Reference Materials of humic acid (HA, Suwannee River humic acid standard II) and fulvic acid (FA, Suwannee River fulvic acid standard) were purchased from the International Humic Substances Society (IHSS). Briefly, aqueous solutions of As(V) were added to HA or FA to prepare for As(V)-HA or As(V)-FA complexes. Similarly, As(V) & Fe (III) solutions were simultaneously added to HA or FA to prepare for As(V)-Fe(III)-HA or As(V)-Fe(III)-FA complexes. The final working standards contained 0.05 mg As/mL and 4 mg HA or FA /mL, with or without 0.2 mg Fe/mL.

Among the SRMs, the As complexed to organic matter, either humic or fulvic acid (As-HA and As-FA, collectively As-HA/FA) and As and Fe bound to either humic or fulvic acid (As-Fe-HA and As-Fe-FA, collectively As-Fe-HA/FA) are the most significant to coals in this study.

2.3.2 Spectra collection

X-ray absorption spectra (XAS) of 5 coals were collected on Beamline 1W1B at the BSRF in July 2014. The spectra of C1 and C3

were collected again on Beamline 4-1 at the Stanford Synchrotron Radiation Light source (SSRL) for inter-laboratory comparison in January 2019 and found to be nearly identical to those collected in July 2014 at BSRF (Fig. S2). The BSRF ring current was 200 mA and the energy was 2.5 GeV, while the SSRL operates at 500 mA and 3 GeV. Both beamlines used Si(220) monochromators with an angle of incident ray or phi angle of 90°, and were detuned 50% to decrease higher-order harmonics and prevent detector saturation. XAS spectra were collected at around the arsenic and iron K-edges, respectively, from -200 to 1000 eV (leading to k range from 0 to 13 Å⁻¹).

Iron spectra were collected using Soller slits and a Mn filter. Fe spectra were calibrated internally using an Fe foil between the second and the third ionization chambers (with an inflection point at 7112.0 eV). Arsenic spectra were calibrated with scorodite (with its edge at 11,874.1 eV). Coal and reference materials were analyzed in fluorescence mode using a Lytle detector at BSRF or a 31-element Ge detector at SSRL. Powdered reference minerals were analyzed in transmission mode. Sample thicknesses were determined based on the quantity of mineral needed to achieve an absorption of 1 μx (37% of light transmitted at the edge, about 10-20 mg over an area of a few cm²). At least three scans were obtained for each sample/reference. No evidence of photooxidation or reduction was observed in successive scans of any coal, or in reference compounds under these analytical conditions.

2.3.3 Data reduction

X-ray absorption near edge spectrum (XANES) and extended X-ray absorption fine structure (EXAFS) spectra were processed using the ATHENA software. For each sample/reference, several collected scans were merged into one, and normalized with linear pre-edge and quadratic post-edge functions and converted to k^3 -weighted chi function as needed. The normalized spectra were then used for either LCF or shell-fitting following methods in our prior studies^{44, 45}.

Briefly, LCFs were performed on: (1) As XANES spectra to determine the oxidation state of As in Guizhou coals; (2) As EXAFS spectra to determine how the As is retained in these coals. For part (1), As XANES LCFs were attempted for energy ranging from -20 to 35 eV using different combinations of arsenopyrite, orpiment, sodium arsenite and scorodite as SRMs (combinations listed in Table S2). For part (2), LCF fits were performed over k -range of 2-12 \AA^{-1} using As(V)-Fe-HA/FA SRMs, sorbed As(V) onto inorganic mineral SRMs, and As-bearing sulphides (combinations listed in Table S2). For each LCF, different combinations of SRMs were all considered in fitting until the best fits were achieved (Fig 1 and Fig S3, Table 1, Table S2 and Table S6). The estimated fit errors of LCF methods are calculated by ATHENA and based on spectral quality, fit quality and similarity between reference spectra, and were typically <5% for each component.

Shell fitting was performed using ATHENA and WinXAS on both Fe and As EXAFS spectra to determine their coordination environments^{46, 47}. This approach used k^3 -weighted EXAFS spectra over a k -range of 2-12 \AA^{-1} and fit in both R-space and k -space. Local structures were determined by varying the coordination number (CN), distance (R , in \AA), disorder as estimated by the Debye-Waller factor (σ^2) for each shell. The coordinating atom (Z) for each shell is inferred based on their unique phase shift and amplitude functions,

which are accurately calculated for different atom-pairs that were calculated using FEFF 7 code. During fitting, E_0 shift were correlated between first and second shell and S_0^2 was fixed to 0.9 for both As and Fe. Other parameters (R , CN, σ^2) were free to change but constrained to positive values.

The number of Fe atoms in body-centered cubic iron clusters is calculated by the equation (1) below based on calculation. We also calculated the n values for coal samples and SRMs based on the CNs determined by Fe EXAFS using also equation (1), under the assumption that Fe clusters in coals and SRMs are also body-centered cubicals.

$$CN = \frac{8*1 + (\sqrt[3]{n}-1)*2 + (\sqrt[3]{n}-1)^2*3 + (\sqrt[3]{n}-1)^3*6}{(\sqrt[3]{n}+1)^3} \quad (1)$$

3. Results and Discussion

3.1 Samples Selected to Represent Permian High-As Guizhou Coal

Five coal samples were selected for XAS analysis on the basis of their similarities in compositions to a larger group of 24 coals collected from Guizhou by this and prior studies^{32, 36} (Table S3). The As, Fe and S concentrations in the 5 coals ranged from 45 to 5,676 mg/kg, 0.6 to 2.1%, and 1.3 to 2.8%, respectively (Table 1). Concentrations of As in coals vary widely worldwide, with frequently cited range between 7 and 4,000 mg/kg²⁹. The sample with the highest As concentration, C4 from Xingren, contained the lowest Fe concentration. No significant correlations between concentrations of As-Fe, As-S and Fe-S are evident among the larger group of coal samples (Table S3).

Likewise, the bulk mineralogy determined by XRD was also similar between the 5 coal samples investigated and the larger group

ARTICLE

(Table 1 and Table S4). Pyrite content ranged from 2% to 7% in the 5 coals (Table 1), while being 1% to 13% in all 24 coals (Table S4). X-ray absorption spectroscopy (XAS) and scanning electron microscopy with energy dispersive X-ray spectroscopy (SEM–EDX) have shown that the most common As species in Cretaceous (145.5 and 65.5 million years before present) coals from Kentucky, Wyoming and Idaho of the USA was pyritic arsenic^{33, 40, 48}. In addition to pyrite, other sulfide minerals including chalcopyrite, sphalerite, orpiment and realgar have also been identified as As-bearing phases in coals from Australia and the US⁴⁹. However, unlike most coals in which sulfidic minerals account for most of As occurrence, it has been demonstrated that pyrite is insufficient to account for the abundant As in Guizhou coals^{30, 31, 36}.

3.2 Arsenic XANES of Guizhou Coals Confirm Oxidized Arsenic

It has been shown that approximately 75% to 100% of As is As(V) in the As K-edge absorption edge of 6 Guizhou coals containing 203 to 32,300 mg/kg As (see Fig. 1 in Ding et al 1999³²). The XANES of 5 coal samples examined here are also indicative of predominantly As(V) mode based on their edge positions of 11874.3 eV (Fig 1b), confirming the earlier though unexplained results in Ding et al 1999³². The XANES peak of As shift towards higher energy level with increasing oxidation state of As in SRMs, from 11,867 eV for nominally zero valent As (as in FeAsS), to 11,871.5 eV for As(III) as in NaAsO₂ and 11,874.0 eV for As(V) as in FeAsO₄ (Fig 1a).

The majority of As (>80%) is present as As(V) in coals C2, C4, C5 based on LCF analysis of their respective As XANES (Table 1). The As XANES spectra of samples C2, C4 and C5 also contain a feature at ~11,868 eV that is easier to tell in the first derivative spectra (Fig 1c) than in the XANES (Fig 1b), indicative of a small fraction (<20%) of

pyritic As or FeAsS (Table 1). Due to the absence of any other peaks in C1 and C3 (Figs 1b and 1c), nearly 100% of As are taken as As(V) without LCF analysis (Table 1). Arsenic EXAFS also support As-O bond with lengths consistent with As(V) and thereby further confirm the dominance of As(V) in Guizhou high-As coals (Fig 2).

We are confident that the prevalence of this As(V) is an accurate representation of the Guizhou coals because the samples contained no evidence of oxidation before or after analysis, and the XANES spectra of C1 and C3 collected in Beijing in 2014 and at Stanford in 2019 are nearly identical (Fig. S2). Coal samples selected for inclusion in this study were based on their lacking any obvious signs of physical or chemical alterations. The reduced pyrite phases are stable, and As in other coals prepared the same way are typically not oxidized^{32, 36}.

3.3 Iron and Arsenic Local Structures in As-Fe-OM Standards

A handful of papers have examined Fe and As local structures by shell fitting of Fe and As EXAFS of ferrihydrite, goethite, scorodite to compare with As-Fe-OM SRMs (Table S5). Most relevant is the As-Fe-OM standard, our shell fitting results of the As-Fe-HA/FA SRMs (Table 2) are consistent with those of Mikutta *et al*¹⁴ (Table S5). All As-FA/HA and As-Fe-HA/FA SRMs have similar first As-O coordination shells at a distance of 1.70 ~ 1.71 Å as expected for arsenate; this is consistent with the K-edge absorption edges of synthetic As(V)-Fe-OM SRMs of As(V)-Fe-HA/FA and As(V)-HA/FA at 11,874.0 eV (Fig 1a).

The Fe EXAFS K-edge spectra of As-Fe-HA and As-Fe-FA standards are nearly identical (Fig 3). Each contains 2 shells, an Fe-O shell near 1.95 Å, and an Fe-Fe shell at ~3.03 Å (Fig 3b). The presence of an Fe-Fe shell is a key indication that Fe atoms are likely oxyhydroxide clusters within the organic matter. Furthermore, the CN_{Fe-Fe} of the Fe-Fe shell decreases from 2.1, 1.6 to 1.3 for goethite,

ferrihydrite and As-Fe-HA SRMs; corresponding to also an estimated decreasing number of Fe atoms (n) as body-centered cubic clusters from 130, 60 to 38 (Table 2).

The similarity between the As K-edge EXAFS spectra of As-Fe-HA and that of As-Fe-FA (Fig. 2) allows us to use just one of them (As-Fe-HA, Table S2) as the SRM for LCF in order to characterize the As structure in coals (Table S2). Furthermore, the As-Fe shells at ~ 3.29 Å are also evident in both As-Fe-HA and As-Fe-FA standards (Fig 2b). The coordination numbers for these As-Fe shells are about 0.7 (Table 2), consistent again with characterization of similar As-Fe-OM ternary complexes (Table S5) by Mikutta et al¹⁴.

3.4 EXAFS of Arsenic in Guizhou Coals Suggest Interactions with Fe-OM

The As EXAFS of the Guizhou coals exhibit similarities to those of FeAsO₄ and As-Fe-OM (HA/FA) and dominated by two shells, an As-O shell and an As-Fe shell (Figure 2). The As-O bond length is 1.68-1.69 Å and is typical for As(V)-O bonds (Table 2), and is much shorter than As(III)-O bonds (1.77Å)⁵⁰. The second-shell of As EXAFS is more informative in terms of how As is retained in these coals. These As(V)-rich coals contain a clear but small As-Fe shell at about 3.28 Å, similar to the distances observed for edge-sharing polyhedra for As adsorbed on Fe oxides⁵¹.

The coordination number of 0.7-0.8 for the As-Fe shell in the coal samples is also consistent with As complexation to iron. This is because these CN_{As-Fe} values are much less than that of scorodite FeAsO₄·2H₂O ($CN_{As-Fe} = 4$), but are nearly identical to coordination numbers determined for synthetic As-Fe-FA and As-Fe-HA complexes used as SRMs ($CN_{As-Fe} = 0.7$, Figure 2b, Table 2). This similarity suggests that As(V) in these coals is also bound to organic matter

through bridging to one or more Fe atoms with further Fe EXAFS evidence described in section 3.5, and not directly complexed by organic matter.

Aside the shell fitting results above, linear combination fitting, which depends on considering a complete and accurate set of SRM spectra (Table S2), provides information about the relative fraction of each SRM in the samples⁵². It is worth noting that As EXAFS spectra of coal samples were best reproduced with combinations of spectra of As-Fe-HA and As-HA complexes as SRMs; using only As adsorbed on inorganic minerals or only As-Sulfur minerals as standards, the fits are very poor (Fig S3, Table S6). Because the combination of As-Fe-HA and As-HA spectra could consistently describe the As EXAFS spectra of all coal samples, without any adsorbed As on inorganic minerals or As-bearing sulfides, implying that these soluble ternary complexes are effective models of the stable As(V)-Fe(III)-OM local structures in coals (Table S6).

3.5 EXAFS of Iron in Guizhou Coals Suggest Small Sized Fe particles

Iron K-edge EXAFS complements the information of As coordination environment inferred from As EXAFS and allows for a more complete characterization of the structure of the As-Fe-OM ternary complexes in these coals. Except for pyritic-Fe in C4, the Fe in four other coals was primarily Fe(III) and had local structures similar to those of ferrihydrite and/or goethite (Fig.3), with interaction with OM further modifying its structure. In these Fe(III)-rich spectra, the first shell observed was attributed to 4-5 oxygen atoms coordinated to Fe at distance 1.98~1.99 Å (Fe-O in Fig.3 and Table 2). This distance is similar to our As-Fe-HA/FA references (and Fe(III) oxyhydroxides with octahedral Fe³⁺,⁵³). The second shell observed was an Fe-Fe shell (edge sharing Fe) at a distance around 3.03 Å, identical to that of ferrihydrite and goethite.

1
2
3 Unlike many other coals containing abundant pyrite⁵⁴⁻⁵⁶, pyrite
4 was evident only in C4 from Xingren whereas C1, C2, C3 and C5 from
5 Anlong all show abundant Fe(III) oxyhydroxides (Fig 3). Fe EXAFS of
6 C4 contain the same shells with pyrite (Fe-S for example at 2.2 Å, and
7 a series of longer Fe-Fe and Fe-S shells) but with lower intensities
8 suggesting that there was an additional component or components
9 that were difficult to isolate. Accordingly, results also indicate that
10 Fe exists as pyrite-like phase in coal C4, while much smaller quantities
11 of pyrite are present in other samples (Table 1) interpreted as
12 representing a new mode of Fe occurrence as discussed below.

13
14
15
16
17
18
19
20
21
22 The CNs of Fe-Fe shells in four coal samples (C1, C2, C3, C5)
23 range from 0.6 to 1.1 (Table 2), significantly smaller than that of As-
24 Fe-HA reference (CN_{Fe-Fe} 1.3), 2-line ferrihydrite (CN_{Fe-Fe} 1.6) and
25 goethite (CN_{Fe-Fe} 2.1). Significant to this study, the CNs are
26 dependent on particle size because small particles have a significant
27 fraction of atoms on surfaces and edges relative to fully coordinated
28 crystallographic sites, and also experience distortion in the crystal
29 that increases disorder³⁴. Thus, this small coordination number
30 indicates that the Fe polymers bound within OM in coals have smaller
31 or similar particle size as As-Fe-HA/FA reference, and must be smaller
32 than even nanoparticles like 2-line ferrihydrite. To evaluate how
33 small these Fe particles can be in coals, we calculate how many Fe
34 atoms are required to achieve such small CNs. Based on the
35 observed Fe-Fe coordination numbers in coals, the Fe(III)
36 oxyhydroxide nanoparticles in these 4 coals contain only 6 to 25 Fe
37 atoms (Table 2), suggesting they are smaller than 2-line ferrihydrite
38 (Fig 4a). The diameters of naturally occurring ferrihydrite particles
39 has been estimated to be 2.4~2.9 nm⁵⁷, supporting our hypothesis of
40 Fe(III)-OM nanoaggregates.

It has also been shown that interaction between Fe and OM
occurs when the ratio of C/(C+Fe) is above 0.89 in laboratory
synthesized DOM/Fe coprecipitates¹⁶. The ratios of C/(C+Fe) of coals
are above 0.9. In addition, we have calculated the site saturation
based on crystal limitations (the number of hydroxyls present on the
surface of iron hydroxides). Based on the number of Fe atoms
calculated from the CNs of Fe-Fe shell and the As/Fe ratio in 4
Guizhou/Anlong coals, C1, C2, C3 and C5, all plot at the bottom of the
line of the theoretically estimated Fe atoms and CN using Equation 1
(Fig 4b). This suggests that As in these four coals are not enough to
cover the surfaces of Fe(III) hydroxides, which implies that surface
sites are also available for organic complexation, supporting our
hypothesis of stabilization of As(V)-Fe(III)-OM nanoaggregates.

3.6 Structural Protection by As(V)-Fe(III)-OM Nanoaggregates

The mechanism responsible for oxidized As(V) in Guizhou coals
containing pyrite remains enigmatic since its discovery more than
two decades ago³⁶. Our spectroscopic characterization of the
Guizhou coals leaves little doubt that both Fe(III) and the As(V) are
stabilized within these coals, likely as As(V)-Fe(III)-OM
nanoaggregates. A ternary complex of As(V) bound through edge-
sharing to small (< 2.4 nm) Fe(III) oxyhydroxide nanoparticles within
the organic matter matrix is reasoned to offer the structural
protection against reduction in the wetland or peatland anoxic
environment encountered by these precursor of coals. XAS analysis
of eight peat profiles (As 3-1800 mg/kg, Fe 90-600 mmol/kg, S 10-
680 mmol/kg) collected from suboxic to reducing environment
revealed large amounts of ferric species, or about 42%-80% of Fe,
and is attributed to stabilization by Fe(III)-NOM complexes⁵⁸.

Complexation of organic matter and with As(V) may be a driving
force in reducing the particle size of Fe(III)-OM nanoaggregates

1 within coal. Organic matter is able to change surface charge density
2 of iron oxides/hydroxides, and therefore affect the aggregation of
3 iron minerals^{5, 35}. Recent lab studies based on XAS, X-ray
4 photoelectron spectroscopy and Infrared spectroscopy have
5 demonstrated that the presence of citrate and As(V) decreases the
6 size of ferrihydrite particles, with reductions in Fe CNs up to 28%⁵⁹.
7
8
9
10
11
12
13
14
15
16
17
18
19
20
21
22
23
24
25
26
27
28
29
30
31
32
33
34
35
36
37
38
39
40
41
42
43
44
45
46
47
48
49
50
51
52
53
54
55
56
57
58
59
60

60. These studies have further confirmed that it is the position of phenol groups rather than the number of phenol groups that controls the interaction between Fe and organic matter, and, in turn, triggers the decrease of CNs of Fe-Fe shell⁶⁰. Other lab studies have also revealed that the interactions between organic ligands like carboxyl group in dissolved organic matter (DOM) and Fe(III) favor formation of Fe minerals with smaller size and thus smaller CNs^{16, 34}. Taken together, these recent lab studies suggest the possibility that natural organic matter may provide protection for Fe(III) reduction during coalification.

Given the long geological time scale for coal formation, the stability of these As(V)-Fe(III)-OM nanoaggregates is amazing and needs attention. We infer that the unusual coordination environment of Fe(III), in which both As(V) and organic carbon protect its surface, helps stabilizing Fe(III) in these coals, although further laboratory and field studies are needed to illuminate the conditions that facilitate the formation of such aggregates, preferably with direct imaging of the structure. Ferric Fe is also stabilized within ferritin, which is a hollow globular protein that holds a number of Fe nanoparticles within an internal cavity, and protects them from reaction. The Fe(III) in ferritin is considerably less reactive relative to free Fe(III) nanoparticles. For example, ferritin-encapsulated Fe(III) has a reduction potential as low as -300 mV at pH 7, much lower than redox potentials needed to reduce isolated Fe(III) nanoparticles of similar structure¹³. The enrichment of free HA

adsorbed on the Cr(III)-HA-Fe colloid surfaces has also been shown to contribute to its stability in recent experimental study⁴. Thus organo-mineral associations may effectively stabilize Fe(III) and As(V) in reducing environments such as anoxic sediment and peat, precursors of coal.

There are a few additional, possible reasons why Fe(III) and As(V) may be stabilized within ternary complexes of coal. First, the largely nonpolar organic matter surrounding the Fe(III) nanoparticles creates a stable low dielectric zone within the pocket, where ions that could reduce Fe(III) are unstable. The presence of large amounts of organic matter on the surface of Fe(III) minerals in these coals also can restrict access of the minerals to microorganisms, thus preventing enzymatic reduction of Fe(III) and associated As(V), although this kinetic effect may be less important over geological time. Further, like the stability of ferritin, the stability of the ternary complex may be a result of the stability of the organic matter conformation conferred by binding to the Fe(III), and possibly the effects of As(V) sorption on surface charge or bridging between particles. Lastly, plants and their litter layers are important sources of organic matter in Guizhou and other coals³⁶. Due to oxygen transport by plants to their roots, not only root Fe(III) plaque is abundant, but also As(V), MMA and DMA are found to be associated with plant roots, even though As(III) is more abundant in reducing soils⁶¹⁻⁶³. Therefore, it is plausible that these As(V) in Guizhou coals may have originated from Fe(III)-plaque abundant in plant roots, and subsequently preserved by As(V)-Fe(III)-OM against reduction throughout the coalification process (See Graphical Abstract).

3.7 Implications for As and Fe mobility in Reducing Environments

It is well known that the geochemical behavior of As is largely controlled by iron minerals, which are ubiquitous on

1
2
3 earth and sensitive to redox process¹³. The reductive dissolution
4 of Fe minerals is considered as one of most important ways for
5 As to release from aquifer sediments to groundwater^{64, 65}.
6
7 Increasingly, studies have begun to investigate how natural
8 organic matters (NOM) interact with Fe and As, with aqueous
9 and solid phase As-Fe-NOM complexes detected in reducing
10 groundwater⁶⁶ and peat⁵⁸, and with enhanced preservation of
11 organic matter observed also in reducing marine sediments⁹. A
12 laboratory study found that the C/(C+Fe) ratios dominated
13 structural compositions and stabilities of Fe-NOM
14 coprecipitates, suggesting that such coprecipitates, with Fe
15 mainly as ferrihydrite, likely increase the resistance of organic
16 matter to microbial decomposition/reduction¹⁶. A subsequent
17 laboratory study confirmed that carbon-rich ferrihydrite
18 polygalacturonic acid-coprecipitates and natural Fe-rich organic
19 flocs contained nanosized clusters of lepidocrocite⁶⁷. In
20 wetlands, Guénet et al.⁷ demonstrated by XAS that nano-
21 lepidocrocite and small Fe clusters bound to NOM existed in
22 wetland soils and the formation of small Fe clusters led to an
23 increased ability for As adsorption. EXAFS studies of U.S. coals
24 from Beulah-Zap, Wyodak-Anderson, and Lewiston-Stockton
25 have shown significant amounts of Fe(III) in coals, although the
26 role of organic matter was not examined, nor the role of trace
27 elements in Fe(III) stabilization⁶⁸. As shown in this study,
28 stabilization of ternary nano-sized arsenate-iron(III)
29 oxyhydroxide-organic matter is possible in coals over geological
30 time scales, it begs the question on whether such
31 nanoaggregates with oxidized forms of Fe and As with OM exist
32 in a much broader ranges of reduced, organic rich sedimentary
33 environment, and in turn, makes Fe and As less mobile.

4. Conclusions

While sulfuric As and reduced Fe species are common in coals worldwide, analyses of the local structures of Fe and As in five representative high-As coals from Guizhou by X-ray absorption spectroscopy suggest a new mode of occurrence as stable arsenate-iron(III) oxyhydroxide-organic matter nanoaggregates. Although this "As(V)-Fe(III)-OM" nanoaggregate system has been observed in laboratory experiments, its occurrence has rarely been reported in natural environment. These As(V)-Fe(III)-OM nanoaggregates in coals likely originate in the plant roots, and preserved throughout the coalification process over geological time scale. Nano-scale structural protection mechanisms of how metals and metalloids interact organic matter to result in thermodynamic disequilibrium in a broad range of reducing environments deserve more attention.

Conflicts of interest

There are no conflicts to declare.

Acknowledgements

Funding for this work was provided from the National Natural Science Foundation of China (Grant # 41772265, #41877505 and #U1612442), US National Science Foundation (NSF) grant EAR 15-21356, and US National Institute of Environmental Health Sciences grant ES010349. Synchrotron data collection was supported by the Beijing Synchrotron Radiation Facility and Stanford Synchrotron Radiation Lightsource. Use of the Stanford Synchrotron Radiation Lightsource, SLAC National Accelerator Laboratory, is supported by the U.S. Department of Energy, Office of Science, Office of Basic Energy Sciences under Contract No. DE-AC02-76SF00515. We thank Drs. Robert B.

Finkelman, Baoshan Zheng, Lirong Zheng and Zhenhua Ding for constructive discussions.

Notes and references

- D. Vantelon, M. Davranche, R. Marsac, C. La Fontaine, H. Guénet, J. Jestin, G. Campaore, A. Beauvois and V. Briois, Iron speciation in iron–organic matter nanoaggregates: a kinetic approach coupling Quick-EXAFS and MCR-ALS chemometrics, *Environmental Science: Nano*, 2019, **6**, 2641-2651.
- J. Ma, H. Guo, L. Weng, Y. Li, M. Lei and Y. Chen, Distinct effect of humic acid on ferrihydrite colloid-facilitated transport of arsenic in saturated media at different pH, *Chemosphere*, 2018, **212**, 794-801.
- H. Guénet, M. Davranche, D. Vantelon, J. Gigault, S. Prévost, O. Taché, S. Jaksch, M. Pédrot, V. Dorcet, A. Boutier and J. Jestin, Characterization of iron–organic matter nano-aggregate networks through a combination of SAXS/SANS and XAS analyses: impact on As binding, *Environmental Science: Nano*, 2017, **4**, 938-954.
- P. Liao, C. Pan, W. Ding, W. Li, S. Yuan, J. D. Fortner and D. E. Giammar, Formation and Transport of Cr(III)-NOM-Fe Colloids upon Reaction of Cr(VI) with NOM-Fe(II) Colloids at Anoxic–Oxic Interfaces, *Environmental Science & Technology (Just Accepted Manuscript)*, 2020, DOI: 10.1021/acs.est.9b07934.
- X. Han, E. J. Tomaszewski, J. Sorwat, Y. Pan, A. Kappler and J. M. Byrne, Effect of Microbial Biomass and Humic Acids on Abiotic and Biotic Magnetite Formation, *Environmental Science & Technology (Just Accepted Manuscript)*, 2020, DOI: 10.1021/acs.est.9b07095.
- Y. Lu, S. Hu, Z. Wang, Y. Ding, G. Lu, Z. Lin, Z. Dang and Z. Shi, Ferrihydrite transformation under the impact of humic acid and Pb: Kinetics, nano-scale mechanisms, and implications for C and Pb dynamics, *Environmental Science: Nano (Just Accepted Manuscript)*, 2019.
- H. Guénet, M. Davranche, D. Vantelon, M. Pédrot, M. Al-Sid-Cheikh, A. Dia and J. Jestin, Evidence of organic matter control on As oxidation by iron oxides in riparian wetlands, *Chemical Geology*, 2016, **439**, 161-172.
- O. S. Pokrovsky, R. M. Manasypov, S. V. Loiko and L. S. Shirokova, Organic and organo-mineral colloids in discontinuous permafrost zone, *Geochimica et Cosmochimica Acta*, 2016, **188**, 1-20.
- W.-W. Ma, M.-X. Zhu, G.-P. Yang and T. Li, Iron geochemistry and organic carbon preservation by iron (oxyhydr)oxides in surface sediments of the East China Sea and the south Yellow Sea, *Journal of Marine Systems*, 2018, **178**, 62-74.
- J. Kus, Application of confocal laser-scanning microscopy (CLSM) to autofluorescent organic and mineral matter in peat, coals and siliciclastic sedimentary rocks — A qualitative approach, *International Journal of Coal Geology*, 2015, **137**, 1-18.
- L. K. ThomasArrigo, C. Mikutta, J. Byrne, K. Barmettler, A. Kappler and R. Kretzschmar, Iron and Arsenic Speciation and Distribution in Organic Flocs from Streambeds of an Arsenic-Enriched Peatland, *Environmental Science & Technology*, 2014, **48**, 13218-13228.
- J. M. Plach, A. V. C. Elliott, I. G. Droppo and L. A. Warren, Physical and Ecological Controls on Freshwater Floc Trace Metal Dynamics, *Environmental Science & Technology*, 2011, **45**, 2157-2164.
- T. Borch, R. Kretzschmar, A. Kappler, P. V. Cappellen, M. Ginder-Vogel, A. Voegelin and K. Campbell, Biogeochemical Redox Processes and their Impact on Contaminant Dynamics, *Environmental Science & Technology*, 2010, **44**, 15-23.
- C. Mikutta and R. Kretzschmar, Spectroscopic evidence for ternary complex formation between arsenate and ferric iron complexes of humic substances, *Environmental Science & Technology*, 2011, **45**, 9550-9557.
- M. Hoffmann, C. Mikutta and R. Kretzschmar, Arsenite binding to natural organic matter: spectroscopic evidence for ligand exchange and ternary complex formation, *Environmental Science & Technology*, 2013, **47**, 12165.
- K. Y. Chen, T. Y. Chen, Y. T. Chan, C. Y. Cheng, Y. M. Tzou, Y. T. Liu and H. Y. Teah, Stabilization of Natural Organic Matter by Short-Range-Order Fe Hydroxides, *Environmental Science & Technology*, 2016, **50**, acs.est.6b02793.
- A. Sundman, T. Karlsson, S. Sjöberg and P. Persson, Complexation and precipitation reactions in the ternary As(V)–Fe(III)–OM (organic matter) system, *Geochimica et Cosmochimica Acta*, 2014, **145**, 297-314.
- L. F. O. Silva, D. Pinto and B. D. Lima, Implications of iron nanoparticles in spontaneous coal combustion and the effects on climatic variables, *Chemosphere*, 2020, **254**, 126814.
- R. B. Finkelman and L. Tian, The health impacts of coal use in China, *International Geology Review*, 2018, **60**, 579-589.
- Z. Hu and S. Gao, Upper crustal abundances of trace elements: A revision and update, *Chemical Geology*, 2008, **253**, 205-221.
- Y. Kang, G. Liu, C. L. Chou, M. H. Wong, L. Zheng and R. Ding, Arsenic in Chinese coals: distribution, modes of occurrence, and environmental effects, *Science of the Total Environment*, 2011, **412-413**, 1-13.
- K. M. Campbell and D. K. Nordstrom, Arsenic Speciation and Sorption in Natural Environments, *Reviews in Mineralogy and Geochemistry*, 2014, **79**, 185-216.
- S. Dai, D. Ren, C. L. Chou, R. B. Finkelman, V. V. Seredin and Y. Zhou, Geochemistry of trace elements in Chinese coals: A review of abundances, genetic types, impacts on human health, and industrial utilization, *International Journal of Coal Geology*, 2012, **94**, 3-21.
- R. B. Finkelman, *Modes of Occurrence of Environmentally-Sensitive Trace Elements in Coal*, Springer Netherlands, 1995.
- R. B. Finkelman, Modes of occurrence of potentially hazardous elements in coal: levels of confidence, *Fuel Processing Technology*, 1994, **39**, 21-34.
- X. Guo, C. Zheng, Y. Liu, J. Liu and X. Lu, The study on the mode of occurrence of mercury, arsenic and selenium in coal, *J Eng Thermophys*, 2001, **22**, 763-766.

- 1
2
3 27. R. Finkelman, Modes of occurrence of trace elements
4 in coal, *US Geological Survey Open-File Report*, 1981,
5 p81-99.
- 6 28. G. Liu, P. Yang, Z. Peng, G. Wang and Z. Cao, Occurrence
7 of trace elements in coal of Yanzhou Mining District,
8 *Geochim (in Chinese)* 2002b, **31**, 85-90.
- 9 29. Y. E. Yudovich and M. P. Ketris, Arsenic in coal: a review,
10 *International Journal of Coal Geology*, 2005, **61**, 141–
11 196.
- 12 30. H. E. Belkin, B. Zheng, D. Zhou and R. B. Finkelman,
13 Preliminary results on the Geochemistry and
14 Mineralogy of Arsenic in Mineralized Coals from
15 Endemic Arsenosis areas in Guizhou Province, P.R.
16 China, *Fourteenth Annual International Pittsburgh Coal
17 Conference & Workshop*, 1997, **23-27**, 1-20.
- 18 31. R. B. Finkelman, H. E. Belkin and B. Zheng, Health
19 impacts of domestic coal use in China, *Proceedings of
20 the National Academy of Sciences*, 1999, **96**, 3427-3431.
- 21 32. Z. Ding, B. Zheng, J. Zhang, H. E. Belkin, R. B. Finkelman,
22 F. Zhao, D. Zhou, Y. Zhou and C. Chen, Preliminary study
23 on the mode of occurrence of arsenic in high arsenic
24 coals from southwest Guizhou Province, *Science China
25 Earth Sciences*, 1999, **42**, 655-661.
- 26 33. G. P. Huffman, F. E. Huggins, N. Shah and J. Zhao,
27 Speciation of arsenic and chromium in coal and
28 combustion ash by XAFS spectroscopy, *Fuel Processing
29 Technology*, 1994, **39**, 47-62.
- 30 34. T. Karlsson and P. Persson, Complexes with aquatic
31 organic matter suppress hydrolysis and precipitation of
32 Fe(III), *Chemical Geology*, 2012, **322-323**, 19-27.
- 33 35. A. M. Vindedahl, J. H. Strehlau, W. A. Arnold and R. L.
34 Penn, Organic Matter and Iron Oxide Nanoparticles:
35 Aggregation, Interactions, and Reactivity,
36 *Environmental Science Nano*, 2016, **3**, 494-505.
- 37 36. Z. Ding, B. Zheng, J. Long, H. E. Belkin, R. B. Finkelman,
38 C. Chen, D. Zhou and Y. Zhou, Geological and
39 geochemical characteristics of high arsenic coals from
40 endemic arsenosis areas in southwestern Guizhou
41 Province, China, *Applied Geochemistry*, 2001, **16**, 1353-
42 1360.
- 43 37. S. Dai and R. B. Finkelman, Coal geology in China: an
44 overview, *International Geology Review*, 2018, **60**, 531-
45 534.
- 46 38. M. Sun, G. Liu, Q. Wu and W. Liu, Speciation analysis of
47 inorganic arsenic in coal samples by microwave-assisted
48 extraction and high performance liquid chromatography
49 coupled to hydride generation atomic fluorescence
50 spectrometry, *Talanta*, 2013, **106**, 8-13.
- 51 39. T. Kanduč, Z. Šlejkovec, N. Mori, M. Vrabec, T.
52 Verbovšek, S. Jamnikar and M. Vrabec, Multielemental
53 composition and arsenic speciation in low rank coal
54 from the Velenje Basin, Slovenia, *Journal of
55 Geochemical Exploration*, 2019, **200**, 284-300.
- 56 40. F. E. Huggins and G. P. Huffman, Modes of occurrence of
57 trace elements in coal from XAFS spectroscopy,
58 *International Journal of Coal Geology*, 1996, **32**, 31-53.
- 59 41. Y. Zhang, S. Li, L. Zheng, J. Chen and Y. Zheng, Evaluation
60 of arsenic sorption and mobility in stream sediment and
hot spring deposit in three drainages of the Tibetan
Plateau, *Applied Geochemistry*, 2017, **77**, 89-101.
42. Y. Meng, G. Gong, D. Wei, Y. Xie and Z. Yin, Comparative
microstructure study of high strength alumina and
bauxite insulator, *Ceramics International*, 2014, **40**,
10677-10684.
43. U. Schwertmann and R. M. Cornell, Iron Oxides in the
Laboratory: Preparation and Characterization, *Wiley,
Weinheim*, 2000.
44. J. Sun, B. J. Mailloux, S. N. Chillrud, A. van Geen, A.
Thompson and B. C. Bostick, Simultaneously quantifying
ferrihydrite and goethite in natural sediments using the
method of standard additions with X-ray absorption
spectroscopy, *Chemical Geology*, 2018, **476**, 248-259.
45. B. C. Bostick, J. Sun, J. D. Landis and J. L. Clausen,
Tungsten Speciation and Solubility in Munitions-
Impacted Soils, *Environmental Science & Technology*,
2018, **52**, 1045-1053.
46. B. Ravel and M. Newville, ATHENA, ARTEMIS,
HEPHAESTUS: data analysis for X-ray absorption
spectroscopy using IFFFIT, *J Synchrotron Radiat*, 2005,
12, 537-541.
47. T. Ressler, WinXAS: a Program for X-ray Absorption
Spectroscopy Data Analysis under MS-Windows,
J.Synchrotron Rad, 1998, **5**, 118-122.
48. F. Huggins, F. Goodarzi and C. Lafferty, *Mode of
Occurrence of Arsenic in Subbituminous Coals*, 1996.
49. A. Kolker, F. E. Huggins, C. A. Palmer, N. Shah, S. S.
Crowley, G. P. Huffman and R. B. Finkelman, Mode of
occurrence of arsenic in four US coals, *Fuel Processing
Technology*, 2000, **63**, 167-178.
50. A. Voegelin and S. J. Hug, Catalyzed oxidation of
arsenic(III) by hydrogen peroxide on the surface of
ferrihydrite: an in situ ATR FTIR study, *Environmental
Science & Technology*, 2003, **37**, 972-978.
51. S. Fendorf, M. J. Eick, P. Grossl and D. L. Sparks, Arsenate
and Chromate Retention Mechanisms on Goethite. 1.
Surface Structure, *Environmental Science & Technology*,
1997, **31**, 315-320.
52. T. Ressler, J. Wong, J. Roos and I. L. Smith, Quantitative
Speciation of Mn-Bearing Particulates Emitted from
Autos Burning (Methylcyclopentadienyl)manganese
Tricarbonyl-Added Gasolines Using XANES
Spectroscopy, *Environmental Science & Technology*,
2000, **34**, 950-958.
53. W. P. Inskeep, R. E. Macur, G. Harrison, B. C. Bostick and
S. Fendorf, Biomineralization of As(V)-hydrous ferric
oxyhydroxide in microbial mats of an acid-sulfate-
chloride geothermal spring, Yellowstone National Park
1, *Geochimica Et Cosmochimica Acta*, 2004, **68**, 3141-
3155.
54. F. Vejjahati, Z. Xu and R. Gupta, Trace elements in coal:
Associations with coal and minerals and their behavior
during coal utilization – A review, *Fuel*, 2010, **89**, 904-
911.
55. K. W. Riley, D. H. French, O. P. Farrell, R. A. Wood and F.
E. Huggins, Modes of occurrence of trace and minor
elements in some Australian coals, *International Journal
of Coal Geology*, 2012, **94**, 214-224.
56. C.-L. Chou, Sulfur in coals: A review of geochemistry and
origins, *International Journal of Coal Geology*, 2012,
100, 1-13.
57. A. C. Cismasu, F. M. Michel, A. P. Tcaciuc, T. Tyliczszak
and J. G. E. Brown, Composition and structural aspects
of naturally occurring ferrihydrite, *Comptes Rendus
Geoscience*, 2011, **343**, 210-218.

Journal Name

ARTICLE

- 1
2
3 58. P. Langner, C. Mikutta and R. Kretzschmar, Arsenic
4 sequestration by organic sulphur in peat, *Nature*
5 *Geoscience*, 2012, **5**, 66-73.
- 6 59. C. Mikutta, J. Frommer, A. Voegelin, R. Kaegi and R.
7 Kretzschmar, Effect of citrate on the local Fe
8 coordination in ferrihydrite, arsenate binding, and
9 ternary arsenate complex formation, *Geochimica et*
10 *Cosmochimica Acta*, 2010, **74**, 5574-5592.
- 11 60. C. Mikutta, X-ray absorption spectroscopy study on the
12 effect of hydroxybenzoic acids on the formation and
13 structure of ferrihydrite, *Geochimica Et Cosmochimica*
14 *Acta*, 2011, **75**, 5122-5139.
- 15 61. T. Sarwar, S. Khan, S. Muhammad and S. Amin, Arsenic
16 speciation, mechanisms, and factors affecting rice
17 uptake and potential human health risk: A systematic
18 review, *Environmental Technology & Innovation*, 2021,
19 **22**, 101392.
- 20 62. A. I. González de las Torres, I. Giráldez, F. Martínez, P.
21 Palencia, W. T. Corns and D. Sánchez-Rodas, Arsenic
22 accumulation and speciation in strawberry plants
23 exposed to inorganic arsenic enriched irrigation, *Food*
24 *Chemistry*, 2020, **315**, 126215.
- 25 63. J. M. Garnier, F. Travassac, V. Lenoble, J. Rose, Y. Zheng,
26 M. S. Hossain, S. H. Chowdhury, A. K. Biswas, K. M.
27 Ahmed, Z. Cheng and A. van Geen, Temporal variations
28 in arsenic uptake by rice plants in Bangladesh: The role
29 of iron plaque in paddy fields irrigated with
30 groundwater, *Science of The Total Environment*, 2010,
31 **408**, 4185-4193.
- 32 64. Y. Zheng, M. Stute, A. van Geen, I. Gavrieli, R. Dhar, H. J.
33 Simpson, P. Schlosser and K. M. Ahmed, Redox control
34 of arsenic mobilization in Bangladesh groundwater,
35 *Applied Geochemistry*, 2004, **19**, 201-214.
- 36 65. L. Rodríguez-Lado, G. Sun, M. Berg, Q. Zhang, H. Xue, Q.
37 Zheng and C. A. Johnson, Groundwater arsenic
38 contamination throughout China, *Science*, 2013, **341**,
39 866-868.
- 40 66. H. Guo, B. Zhang and Y. Zhang, Control of organic and
41 iron colloids on arsenic partition and transport in high
42 arsenic groundwaters in the Hetao basin, Inner
43 Mongolia, *Applied Geochemistry*, 2011, **26**, 360-370.
- 44 67. L. K. ThomasArrigo, J. M. Byrne, A. Kappler and R.
45 Kretzschmar, Impact of Organic Matter on Iron(II)-
46 Catalyzed Mineral Transformations in Ferrihydrite–
47 Organic Matter Coprecipitates, *Environmental Science &*
48 *Technology*, 2018, **52**, 12316-12326.
- 49 68. S. R. Wasserman, R. E. Winans and R. McBeth, Iron
50 Species in Argonne Premium Coal Samples: An
51 Investigation Using X-ray Absorption Spectroscopy,
52 *Energy & Fuels*, 1996, **10**, 392-400.
- 53 69. W. P. Inskeep, R. E. Macur, G. Harrison, B. C. Bostick and
54 S. Fendorf, Biomineralization of As(V)-hydrous ferric
55 oxyhydroxide in microbial mats of an acid-sulfate-
56 chloride geothermal spring, Yellowstone National Park,
57 *Geochimica et Cosmochimica Acta*, 2004, **68**, 3141-
58 3155.
- 59
60

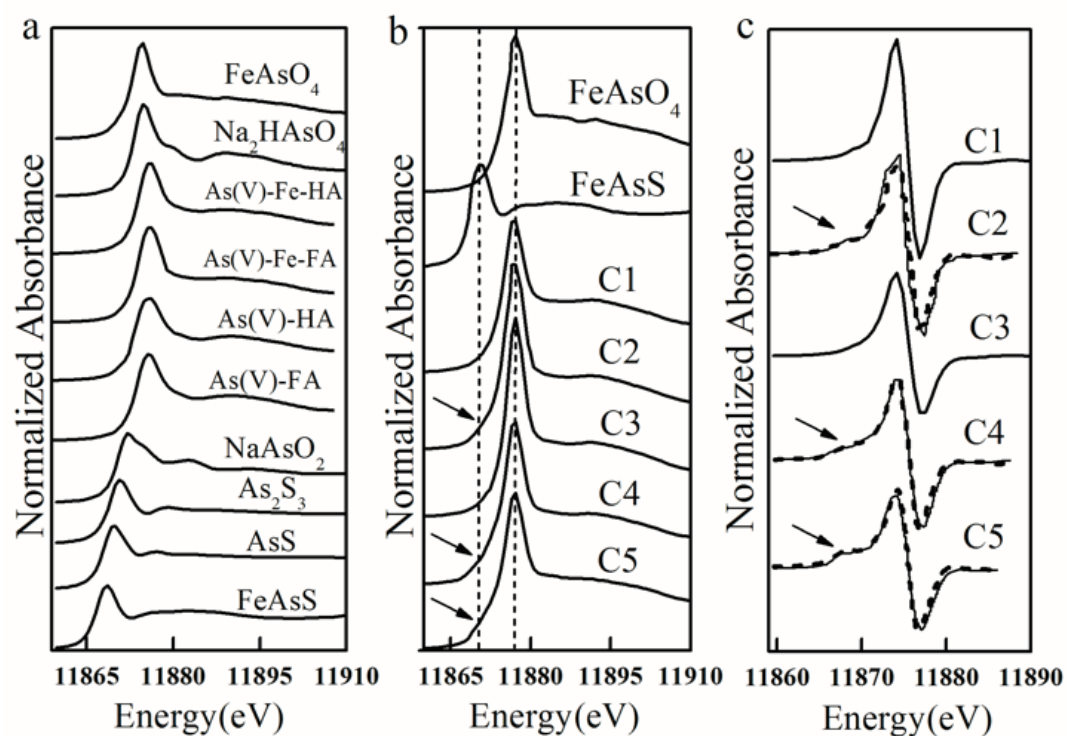


Fig.1 XANES spectra of (a) compounds used as As standards and synthetic As-Org(HA/FA) and As-Fe-Org(HA/FA) standards (b) 5 coal samples with 2 standard As compounds ($\text{FeAsO}_4(\text{V})$, $\text{FeAsS}(0)$) that share the same position of absorption edge as that of samples, and (c) linear combination fits (dashed lines) for coals (C2, C4, C5) in the first-derivative of XANES (Table 1). Coal samples C1 and C3 (fits not shown) are 100% As(V) (Table 1).

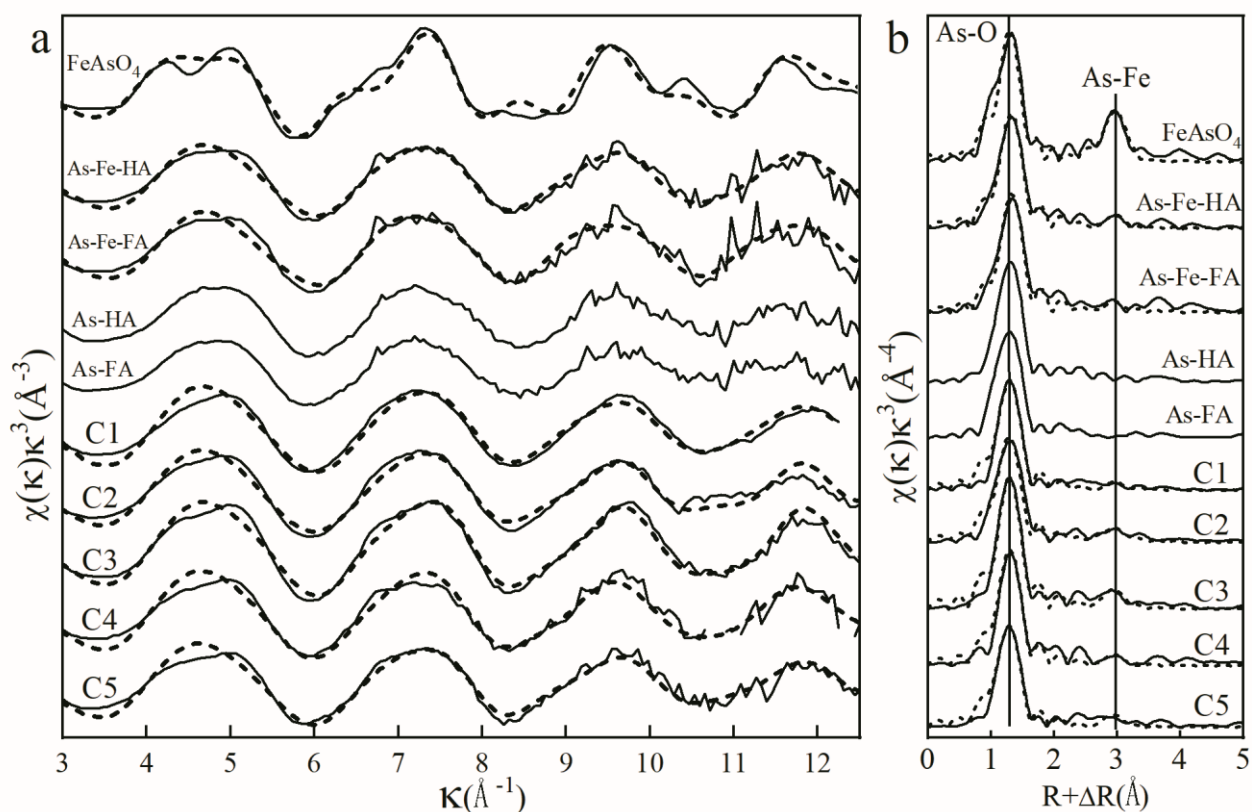


Fig.2 Arsenic K-edge EXAFS spectra with (a) k^3 -weighted fitting in k -space for five coal samples and As-Fe-HA/FA standards and (b) peak fits for coal samples and As-Fe-HA/FA standards in R -space. As-Fe shells are absent in standards of As-HA/FA (fits not shown). Solid lines represent data, and dash lines represent As-O and As-Fe path fitting results (Table 2).

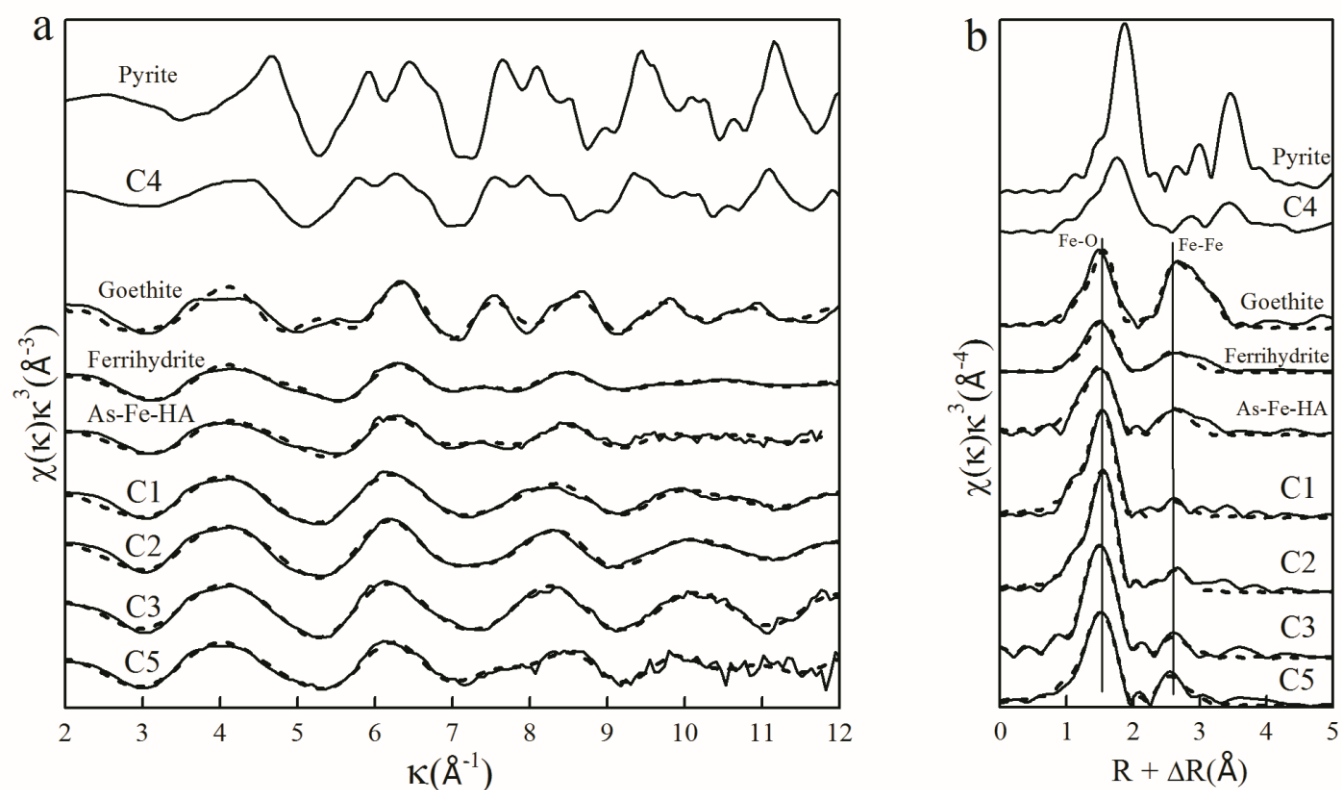


Fig.3 Iron K-edge EXAFS spectra with (a) k^3 -weighted fitting in k -space for coal samples (C1, C2, C3, C5) and three standards (goethite, ferrihydrite and As-Fe-HA), sample C4 and pyrite, (b) peak fits in R -space for coal samples (C1, C2, C3, C5) and three standards (goethite, ferrihydrite and As-Fe-HA), sample C4 and pyrite. Solid lines represent data, and dash lines represent Fe-O and Fe-Fe path fitting results (Table 2).

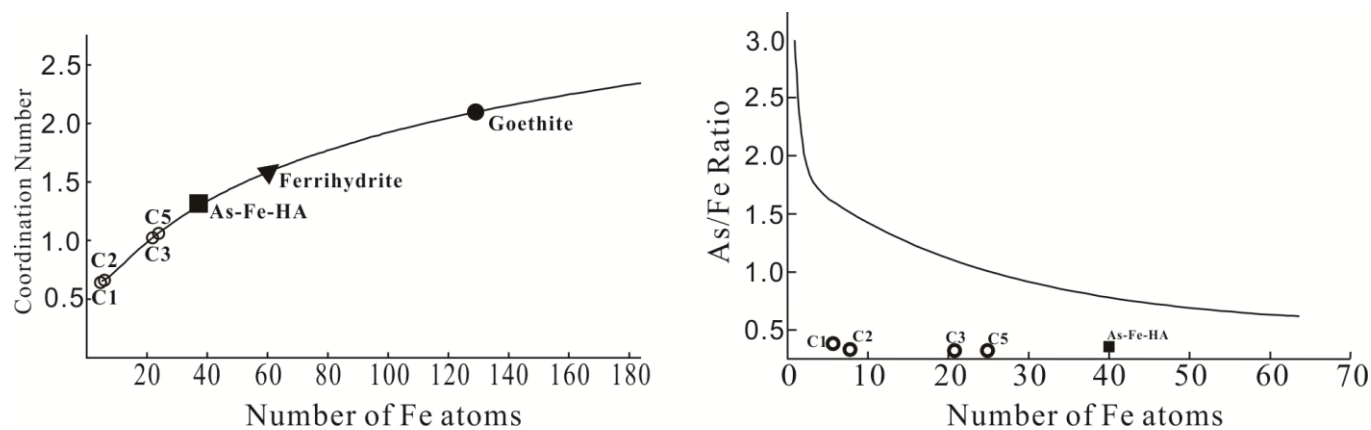


Fig.4 Theoretically calculated coordination numbers (CNs) of Fe-Fe shell increases with the increase of Fe atoms in an iron cluster (based on Inskeep et al⁶⁹). The hollow circles (4 Guizhou coal samples) show CNs determined by Fe EXAFS (left) and molar ratio of As/Fe (right).

ARTICLE

Table 1 Bulk minerology, concentrations of Fe, C, S and As, and speciation of As in five Guizhou coals from China

Sample	Chemical and Mineral Compositions							Arsenic Species				
	Fe ^b (mg/kg, ICPOES)	C (%, Elements analyser)	S (%,Elements analyser)	Ill (%, XRD)	Kao (%, XRD)	Hem (%, XRD)	Py (%, XRD)	As _(Total) (mg/kg, HG-AFS)	As(V)(%)	As(III) (%)	As- Sulfide (%)	R-factor ^a
ML-1(C1)	10928	60.2	1.6	28	12	2	4	5676	100 ^c	-	-	-
JL-92(C2)	7859	76.2	2.8	24	26	2	7	175	85±5 ^b	9±6 ^b	6±5 ^b	0.006
LC-1(C3)	15480	64.5	1.7	17	23	n.d ^a	2	698	100 ^c	-	-	-
GCO-5(C4)	21733	56.7	1.9	18	15	4	4	45	86±4 ^b	2±3 ^b	12±4 ^b	0.004
Hz-Au-97(C5)	6885	66.2	1.3	23	22	<1	2	111	81±5 ^b	5±4 ^b	14±5 ^b	0.005

^a R-factor represents the relative error of the fit and data

^b calculated from LCF of XANES

^c There is only one peak at position of As(V) in XANES for C1 and C3 (Fig 1), 100% of As(V) is assumed.

Table 2. Arsenic and Fe local structures for selected model compounds and coals.

		path	CN ^a	R ^b	σ^{2c}	path	CN ^a	Number of Fe atoms ^d	R ^b	ΔE_0 (eV) _g	σ^{2c}
As K-edge											
Model compounds	FeAsO ₄ ·2H ₂ O	As-O	4.0	1.69	0.002	As-Fe	4.1	--	3.30	1.58	0.006
	As(V)-Fe-HA	As-O	3.7	1.70	0.002	As-Fe	0.7	--	3.29	5.54	0.003
	As(V)-Fe-FA	As-O	3.8	1.71	0.002	As-Fe	0.7	--	3.29	5.19	0.005
	As(V)-HA	As-O	3.8	1.69	0.002	As-Fe	-- ^e	--	-- ^e	--	-- ^e
	As(V)-FA	As-O	3.8	1.69	0.002	As-Fe	-- ^e	--	-- ^e	--	-- ^e
Coal samples	C1	As-O	3.9	1.69	0.003	As-Fe	0.7	--	3.27	6.58	0.004
	C2	As-O	3.8	1.69	0.003	As-Fe	0.7	--	3.29	6.57	0.002
	C3	As-O	4.0	1.68	0.002	As-Fe	0.8	--	3.28	5.62	0.003
	C4	As-O	3.9	1.69	0.004	As-Fe	0.7	--	3.28	5.86	0.005
	C5	As-O	4.0	1.69	0.002	As-Fe	0.8	--	3.26	4.32	0.006
Iron K-edge											
Model compounds	Goethite	Fe-O	3.0	1.98	0.005	Fe-Fe	2.1	130	3.03	3.71	0.005
	Ferrihydrite	Fe-O	3.1	1.98	0.005	Fe-Fe	1.6	60	3.03	3.62	0.009
	As-Fe-HA	Fe-O	4.5	1.98	0.008	Fe-Fe	1.3	38	3.04	2.65	0.007
Coal samples	C1	Fe-O	5.1	1.99	0.006	Fe-Fe	0.6	6	3.03	3.54	0.006
	C2	Fe-O	5.3	1.99	0.006	Fe-Fe	0.7	8	3.05	2.89	0.003

ARTICLE								Journal Name			
C3	Fe-O	5.2	1.99	0.005	Fe-Fe	1.0	21	3.05	3.46	0.005	
C4 ^f	--	--	--	--	--	--	--	--	--	--	
C5	Fe-O	5.3	1.98	0.008	Fe-Fe	1.1	25	3.04	3.30	0.004	

^a coordination number;

^b path length (Å), the interatomic distance R within 0.01 Å, ;

^c Debye-Waller parameter;

^d Numbers of Fe atoms are calculated based on CNs of Fe-Fe shells (Fig 4, calculation method is provided in method);

^e The "As-Fe" shell is either absent or undetectable under certain coordination numbers in As-HA/FA standards;

^f Iron structure in C4 is like that of pyrite(Fig.3b), the Fe-Fe shell is not obvious.

^g Energy shift parameter